# Semibatch RAFT Polymerization for Branched Polyacrylamide Production: Effect of Divinyl Monomer Feeding Policies

**Dunming Wang, Wen-Jun Wang, and Bo-Geng Li**
State Key Laboratory of Chemical Engineering, Institute of Polymerization and Polymer Engineering, Dept. of Chemical and Biological Engineering, Zhejiang University, Hangzhou, Zhejiang 310027, P.R. China

**Shiping Zhu**
Dept. of Chemical Engineering, McMaster University, Hamilton, ON, Canada L8S 4L7

*DOI 10.1002/aic.13890*
*Published online August 6, 2012 in Wiley Online Library (wileyonlinelibrary.com).*

*Star and hyperbranched polyacrylamides (s-PAMs and b-PAMs) were synthesized via semibatch RAFT copolymerization of acrylamide (AM) and N,N′-methylenebisacrylamide (BisAM) using four monomer feeding policies. The BisAM to chain transfer agent (CTA) ratios from 1 to 40 at a constant $[AM]_0/[CTA]_0$ of 600 were investigated at 60°C. The s-PAMs with the number of arms of 1.4–12.8 and 1.8–8.4 were, respectively, produced by arm-first (AF) and core-first (CF) approaches, whereas the b-PAMs having the branching density of 1.34–13.1C/1000Cs were synthesized by constant BisAM feeding (semibatch polymerization, SB) and batch (batch polymerization, BA). Soluble b-PAMs were produced with the four feeding policies at $[BisAM]_0/[CTA]_0$ of 5. However, when the $[BisAM]_0/[CTA]_0$ was increased to 30, the gelation occurred with the CF and BA approaches while the AF and SB synthesized soluble branched PAMs. The AF and SB approaches appeared to be practical in producing the respective s-PAM and b-PAM at high $[BisAM]_0/[CTA]_0$ ratios or low CTA usages.*  *AIChE J,* 59: 1322–1333, 2013
*Keywords: polymerization, polymer properties, monomer feeding policies, star polyacrylamide, hyperbranched polyacrylamide*

## Introduction

Water-soluble polymers have been widely used as flocculants for solid–liquid separation in wastewater treatment, as well as many other areas such as pulp and paper, mineral processing, and oil recovery.[1–4] Acrylamide polymers (PAMs) including homopolymers and copolymers are the most popular flocculants.[2] The polymer structure, molecular weight (MW), and charge density in the case of polyelectrolytes determine the flocculation efficiency.[3] It is known that the flocculation effect increases with MW of PAMs.[5] High MWs ($>10^6$ g/mol) are often required in industrial applications. However, high-MW polymers have high viscosities and are thus time-consuming in preparation of aqueous solutions. There were several literatures reporting that PAMs including highly branched, star, and brush structures had higher flocculation efficiencies than linear counterparts and at the same time were readily soluble.[6–13] For example, Zhu and coworkers prepared graft cationic polyelectrolytes and found that the graft polymers performed better in flocculation applications than their linear counterparts.[9–13]

Branched polymers are those having graft, star, comb, hyperbranched, and dendritic structures. Star and hyperbranched polymers attract great attention because of their unique rheological and physical properties.[14,15] These structures can be synthesized by different feeding policies using various vinyl monomers. Of particular interest is the recent development of controlled/"living" radical polymerization (CLRP) processes that provide easy ways to prepare these branched polymers by copolymerization of monomers with multifunctional comonomers such as divinyl monomers.[14–20] Star polymers are usually prepared by "arm-first" (AF) or "core-first" (CF) approaches. In an AF approach, linear polymer chains are synthesized first and serve as arm precursors. These arms are attached each other via copolymerization with divinyl comonomers. The resulting star polymers have the number of arms with a statistical distribution and a highly cross-linked core. In contrast, in a CF approach, divinyl monomers copolymerize first by CLRP to generate nanogels, which contain multifunctional groups. The nanogels act as multifunctional cores and undergo consecutive growth of arms via further polymerization of added monomer. The number of arms in the star polymers also follows a statistical distribution.[21] If divinyl monomers are continuously fed into a reactor, either at a constant rate or varying rates (semibatch polymerization or SB)[22,23] or are added in batch (batch polymerization or BA),[24–38] the divinyl monomers copolymerize with monomers and generate branches along polymer chains, resulting in hyperbranched structures.

Various well-defined star and hyperbranched polymers have been synthesized by RAFT polymerization via these feeding policies. Reversible addition-fragmentation chain

Correspondence concerning this article should be addressed to W.-J. Wang at wenjunwang@zju.edu.cn or S. Zhu at zhuship@mcmaster.ca.

transfer (RAFT) polymerization is proven to be an effective method to prepare the branched structures. Using an AF approach, Davis and coworkers introduced divinylbenzene (DVB) into copolymer chains to form linear polystyrene-*b*-polydivinylbenzene (PS-*b*-PDVB) block copolymers via RAFT polymerization.[39] A successive free radical polymerization coupled pendent vinyl groups in the PDVB blocks to form core-crosslinked stars with up to 16 arms. Zheng and Pan[40] prepared PS and PS-*b*-poly(*N*-isopropyl acrylamide) (NIPAM) star polymers via RAFT polymerization of St and its successive polymerization with NIPAM followed by copolymerization with DVB. The same method was used to synthesize poly(acrylic acid) stars with fluorescent divinyl comonomer core,[41] poly(N-isopropyl acrylamide) (PNIPAM) or poly(2-hydroxyethylmethacrylate) stars with ethyleneglycol dimethacrylate or DVB core,[42] and poly(ethylene oxide) stars with St/DVB microgel core.[43]

Although star polymers could also be synthesized via CF approaches with divinyl monomers, there are few reports in the literature using controlled radical polymerization (CRP) methods. Gao and Matyjaszewski[21] used atom transfer radical polymerization (ATRP) of ethyleneglycol diacrylate to form a multifunctional crosslinked core for further synthesis of polyacrylate stars. Other CF star polymers were mainly prepared using multifunctional initiators,[44–52] chain transfer agents (CTAs),[53–67] or coupling agents.[60,68–71] Using batch RAFT polymerization, hyperbranched polymers could be readily synthesized through copolymerization with divinyl monomer in the presence of CTA.[28–33,36,38] In our previous work,[22,23] we reported a semibatch RAFT polymerization method with continuous feeding of *N*,*N*′-methylenebisacrylamide (BisAM) to synthesize hyperbranched polyacrylamide (b-PAM) via 3-benzyltrithiocarbonyl propionic acid (BCPA) as CTA.

Despite that each of the feeding policies has been applied to synthesize various star and hyperbranched polymers, there is no systematic study to assess their performances with a same monomer system. Therefore, their relative advantages and disadvantages are not known in terms of branching efficiencies. Most discussions in the literature are not directly supported by experimental data. In this work, we provide a direct comparison of all these four feeding policies in the RAFT copolymerization of AM/BisAM and demonstrate their effects on the synthesis of s- or b-PAMs. Scheme 1 shows the synthetic routes and their corresponding monomer feeding policies.

## Experimental Section

### *Materials*

Acrylamide (AM, ≥98.5%) was purchased from Lingfeng Chemical Reagent, China. Ammonium persulfate (APS, 98%) and BisAM (≥98%) were obtained from Sinopharm Chemical Reagent, China. AM and BisAM were recrystallized in acetone and ethanol, respectively, prior to use, whereas APS was used as received. BCPA was synthesized according to the literature.[72]

### *Synthesis of star polyacrylamide by "arm-first" RAFT polymerization (AF)*

A clean and dry flask equipped with a mechanical stirrer was charged with AM (7.1 g, 0.1 mol), BCPA (45.3 mg, $1.67 \times 10^{-4}$ mol), and sodium acetate/acid acetate buffer solution (100 g, pH = 5), deoxygenated by $N_2$ for at least 30 min and heated to 60°C. The APS (19.0 mg, $8.37 \times 10^{-5}$ mol) was then injected to initiate the polymerization. After AM was polymerized for 4 h to reach a high conversion, a pre-prepared and deoxygenated BisAM solution (0.128–1.03 g or 8.33–66.7 $\times 10^{-4}$ mol of BisAM in 50 g deionized water) was added in batch the reactor to copolymerize with the linear PAM arms.

### *Synthesis of star polyacrylamide by core-first" RAFT polymerization (CF)*

A small amount of BisAM (0.0256–0.770 g or 1.67–$50.0\times10^{-4}$ mol) was added into a flask together with BCPA (45.3 mg, $1.67 \times 10^{-4}$ mol) and buffer solution (50 g, pH = 5). The system was heated to 60°C after deoxygenated by $N_2$ for at least 30 min, and then APS (19.0 mg, $8.37 \times 10^{-5}$ mol) was injected. The BisAM was polymerized at 60°C for 3 h to form nonprecipitated nanogels before the AM solution (7.1 g or 0.1 mol of AM dissolved in 50 g buffer solution and 50 g deionized water, and deoxygenated by $N_2$) was added. The copolymerization of AM with the nanogels was continued for another 5 h.

### *Synthesis of b-PAM by RAFT polymerization with constant feeding of BisAM (SB)*

AM (7.1 g, 0.1 mol), buffer solution (100 g, pH = 5), and BCPA (0.0453 g, $1.67 \times 10^{-4}$ mol) were added into a flask equipped with a mechanical stirrer. A certain amount of BisAM (0.128–1.03 g or 8.33–$66.7\times10^{-4}$ mol) was dissolved in 50 g of deionized water and inhaled in a syringe equipped to a micrometering pump. After deoxygenated by $N_2$ for at least 30 min, the polymerization system was heated to 60°C, and APS (19 mg, $8.37 \times 10^{-5}$ mol) was injected to the flask to initiate the polymerization. The BisAM solution was then fed to the system at a constant rate of 16.7 mL/h. Upon completion of BisAM addition, the polymerization was continued for additional 30 min prior to termination by cooling.

### *Synthesis of b-PAM by batch RAFT polymerization (BA)*

AM (7.1 g, 0.1 mol), BCPA (0.0453 g, $1.67 \times 10^{-4}$ mol), buffer solution (100 g, pH = 5), deionized water (50 g), and BisAM (0.128–0.77 g or 8.33–$50.0\times10^{-4}$ mol) were added to a flask equipped with a mechanical stirrer in one batch. The system was deoxygenated by $N_2$ for at least 30 min and heated to 60°C before APS (19 mg, $8.37 \times 10^{-5}$ mol) was injected to start the polymerization. The polymerization was conducted for 3.5 h or stopped when the system gelled.

### *Characterization*

Monomer conversions were determined from the residual monomer concentrations in the samples using an Agilent 6890N gas chromatograph equipped with an Agilent 7683B series injector, a flame ionization detector, and a capillary column (HP-5, 30 m × 0.32 mm × 0.25 μm). Nitrogen as carrier gas was controlled at 1 mL/min under 0.5 MPa. The injection port was set at 250°C. The GC column was programmed as follows: staying at 100°C for 3 min, then increasing to 250°C at a heating rate of 40°C/min and remaining at 250°C for 1 min. The MWs of PAM samples were characterized using a Polymer Laboratory PL-GPC 50 gel permeation chromatography (GPC) with differential refractive index, viscometer (IV), and laser light scattering (LS) triple detectors in series. The LS detection angle was 90°, and the laser wavelength was 650 nm. A series of PL-aquagel-60, PL-aquagel-40, and PL-aquagel-20 columns were equipped in the GPC. $NaNO_3$ aqueous solution (0.1 N) was used as eluent at a flow rate of 0.8 mL/min and 30°C.

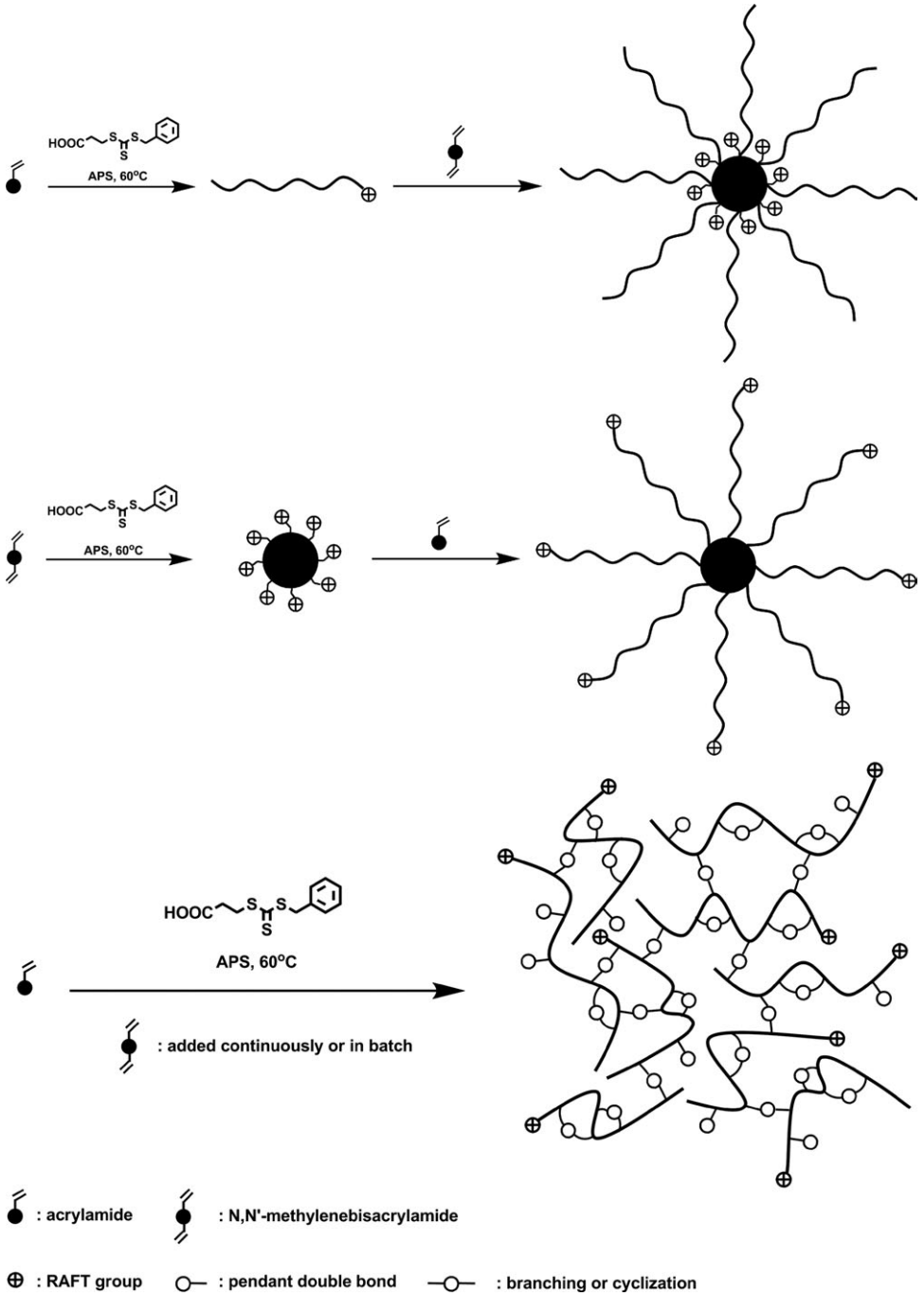


**Scheme 1. Synthetic route of s-PAM and b-PAM using RAFT copolymerization of AM with BisAM via AF, CF, constant feeding (SB), and batch (BA) approaches.**

The calibrations were conducted against five poly(ethylene oxide) (PEO) standards ($MW_1 = 1190$ kg/mol, $PDI_1 = 1.21$; $MW_2 = 162$ kg/mol, $PDI_2 = 1.45$; $MW_3 = 89$ kg/mol, $PDI_3 = 1.26$; $MW_4 = 0.6$ kg/mol, $PDI_4 = 1.06$; as well as a PEO mixed standard having MW from 2 to 162 kg/mol). The *dn*/*dc* values of PAM and PEO were 0.170 and 0.133 mL/g, respectively.[73] The delay volumes IDD between the detectors were determined by PEO standards with 0.110 mL for LS and −0.562 mL for IV. $^1$H NMR spectra were acquired on a Bruker Advance 400 spectrometer with $D_2O$ as solvent. In the $^1$H NMR spectrum, two peaks at 1.5 and 2.0 ppm with a 2 to 1 integral intensity ratio were attributed to methylene and methine in PAM backbone. The peaks at 6.8 and 7.5 ppm were resulted from the pendant double bonds of BisAM with one vinyl reacted, suggesting that not all reacted BisAM contributed to branching. The detailed estimation of the content of residual pendant vinyl groups ($c_p$) from the $^1$H NMR spectrum has been presented in Ref. 23.

## Results and Discussion

Star polyacrylamides (s-PAMs) and b-PAMs were synthesized with four different feeding strategies of BisAM under various molar ratios of BisAM to AM from 0.0017 to 0.067. The experimental recipes for all the runs are summarized in Table 1. The overall and monomer conversions, weight-

**Table 1. Receipts for Synthesis of s-PAMs and b-PAMs**

| | Run | | | | | | | | | | | | |
|---|---|---|---|---|---|---|---|---|---|---|---|---|---|
| | AF5 | AF20 | AF30 | AF40 | CF1 | CF3 | CF5 | CF30 | BA5 | BA30 | SB5 | SB30 | SB40 |
| [AM] (mol/L) | | | | | | | 0.667 | | | | | | |
| [BisAM] (mmol/L) | 5.56 | 22.3 | 33.5 | 44.6 | 1.11 | 3.34 | 5.56 | 33.5 | 5.56 | 33.5 | 5.56 | 33.5 | 44.6 |
| [CTA] (mmol/L) | | | | | | | 1.11 | | | | | | |
| [I] (mmol/L) | | | | | | | 0.558 | | | | | | |

average MW ($M_w$), polydispersity indexes (PDIs), intrinsic viscosities, and contraction factors of the PAM samples are summarized in Table 2. Soluble PAMs were produced in all the runs except for Runs CF30 and BA30, with a total monomer conversion over 93.5%. The s-PAMs had $M_w$ of 82.3–715 kg/mol and PDI of 1.1–2.4, whereas the b-PAMs' $M_w$s and PDIs were 100–1290 kg/mol and 1.4–9.4, respectively.

From $^1$H NMR spectra of the PAM samples, the contents of unreacted pendant double bonds ($c_p$) contributed by BisAM were determined. The $c_p$ values were 0.07–0.97% of the total reacted vinyl groups (from both reacted AM and reacted BisAM) in the s-PAMs and 0.49–1.02% in the b-PAMs. The fractions of the pendent double bonds over the total incorporated BisAM monomers ($f_p$) having one or both vinyl groups reacted were estimated using the expression in Ref. 23 and listed in Tables 2 and 3. It can be seen that 53.7–85.5% of the incorporated BisAMs had both vinyl groups crosslinked to form the s-PAMs, whereas 42.4–82.9% of the BisAM monomers participated in branching or cyclization contributing to the formation of the b-PAMs.

Star and branched polymers have lower root mean-square gyration radius $\left\langle R_g^2 \right\rangle^{1/2}$ and intrinsic viscosity ([$\eta$]) than their linear counterparts of the same MW due to the shrinking effect,[15,74–76] which can be described by the contraction factors $g$ and $g'$. For linear PAMs, there exist the following equations with $[\eta] = 1.12 \times 10^{-4} M^{0.769}$ and $\left\langle R_g^2 \right\rangle^{1/2} = 1.70 \times 10^{-2} M^{0.583}$.[23] The $g$ and $g'$ data were found as 0.214–0.894 and 0.332–0.931, respectively, for the s-PAMs and 0.194–0.889 and 0.283–0.915 for the b-PAMs. There exists a quantitative relationship between $g$ and $g'$ with

$$g' = g^{\varepsilon} \tag{1}$$

where $\varepsilon$ is an exponential factor. The $\varepsilon$ was 0.74 for the b-PAMs.[23] From the $g$ and $g'$ values in Table 2, the $\varepsilon$ value for the s-PAMs was determined to be 0.62, which is close to the value of 0.5 for nonfree drain regular stars.[75] The $\varepsilon$ values were used for further estimation of the number of arms for the s-PAMs and the branching density for the b-PAMs from $g'$.

### *Number of arms and distribution in the s-PAMs synthesized by AF approach*

Four different BisAM to CTA ratios of 5 (AF5), 20 (AF20), 30 (AF30), and 40 (AF40) (equivalently, BisAM to AM ratios of 0.0083, 0.033, 0.050, and 0.067) were used to produce the s-PAM samples with the AF method. As the arm precursors, the AM monomers were polymerized to achieve high conversion first. Each PAM precursor chain bore a —SC(Z)=S moiety at its chain end from the CTA. The BisAM monomers were copolymerized through chain extension, resulting in the formation of crosslinked cores. Therefore, the ratio of BisAM/CTA also corresponded to that of BisAM molecules to the PAM precursor chains. Runs AF5–AF40 had the AM conversions of 94.2–97.3% in the arm formation step. The s-PAMs had $M_w$s of 82.3–715 kg/mol and PDIs of 1.1–2.2 with the overall conversions of 97.1–98.1%.

Figure 1 shows the GPC traces of the s-PAM samples from Runs AF5–AF40. There appeared to have two major

**Table 2. Synthesis and Characterization of s-PAMs and b-PAMs Using RAFT Copolymerization***

| Run | $[BisAM]_0/[CTA]_0$ | $x_1$† (%) | $x$† (%) | $x_{AM}$† (%) | $x_{BisAM}$† (%) | $M_w$ (kg/mol) | PDI | [$\eta$] (dL/g) | $g'$‡ | $g$‡ | $c_p$§ (%) |
|---|---|---|---|---|---|---|---|---|---|---|---|
| s-PAMs | | | | | | | | | | | |
| AF5 | 5 | 94.3 | 97.1 | 97.1 | 98.2 | 82.3 | 1.1 | 0.480 | 0.931 | 0.894 | 0.36 |
| AF20 | 20 | 94.2 | 97.8 | 97.7 | 98.8 | 175 | 1.7 | 0.548 | 0.806 | 0.726 | 0.51 |
| AF30 | 30 | 97.3 | 98.1 | 98.0 | 99.1 | 324 | 2.2 | 0.568 | 0.585 | 0.452 | 0.67 |
| AF40 | 40 | 96.7 | 97.7 | 97.4 | 99.4 | 715 | 2.2 | 0.562 | 0.332 | 0.214 | 0.97 |
| CF1 | 1 | 80.6 | 96.4 | 96.4 | 99.9 | 108 | 1.6 | 0.571 | 0.875 | 0.809 | 0.07 |
| CF3 | 3 | 65.7 | 96.5 | 96.5 | 99.9 | 238 | 1.7 | 0.587 | 0.738 | 0.618 | 0.23 |
| CF5 | 5 | 56.7 | 97.6 | 97.6 | 99.9 | 579 | 2.4 | 0.796 | 0.552 | 0.398 | 0.39 |
| CF30 | 30 | Gel | | | | | | | | | |
| b-PAMs | | | | | | | | | | | |
| BA5 | 5 | | 93.5 | 93.4 | 99.6 | 204 | 1.9 | 0.561 | 0.801 | 0.745 | 0.49 |
| BA30[22] | 30 | | Gel | | | | | | | | |
| SB5 | 5 | | 94.5 | 94.4 | 99.9 | 100 | 1.4 | 0.473 | 0.915 | 0.889 | 0.59 |
| SB30[23] | 30 | | 95.2 | 94.6 | 99.9 | 1278 | 8.4 | 0.892 | 0.301 | 0.210 | 0.94 |
| SB40 | 40 | | 98.8 | 98.8 | 99.1 | 1290 | 9.4 | 0.773 | 0.283 | 0.194 | 1.02 |

*AM concentration $[AM]_0$ was 1 mol/L. BCPA and APS were used as CTA and initiator (I) respectively. $[AM]_0/[CTA]_0/[I]_0$ was kept at 600/1/0.5 in all runs. All the runs were carried out in buffer solutions of pH = 5 at 60°C.
†$x$, $x_{AM}$, and $x_{BisAM}$: conversions of total monomers, AM, and BisAM, respectively. $x_1$: monomer conversion at first stage polymerization when AF and CF approaches used to produce b-PAMs.
‡$g'$ and $g$ were weight-average contraction factors.
§$c_p$: molar ratio of pendant double bond to polymerized vinyl units calculated from $^1$H NMR spectra.

**Table 3. The Number of Arms and the Fraction of BisAM with Both Vinyl Groups Contributed to the Core Formation Determined by $^1$H NMR, Triple-Detector GPC and Fractionation of GPC Traces for the s-PAMs**

| Run | $[BisAM]_0/[CTA]_0$ | $N_p$* | $N_g$† | $N_{PF}$‡ | $f_p$§ (%) | $f_c$§ (%) |
|---|---|---|---|---|---|---|
| AF5 | 5 | 1.4 | 1.5 | 1.5 | 42.8 | 57.2 |
| AF20 | 20 | 3.2 | 3.3 | 3.7 | 16.1 | 83.9 |
| AF30 | 30 | 5.6 | 5.9 | 5.8 | 14.5 | 85.5 |
| AF40 | 40 | 12.8 | 13.3 | 13.2 | 16.0 | 84.0 |
| CF1 | 1 | 1.8 | 1.7 | 1.5 | 40.6 | 59.4 |
| CF3 | 3 | 3.3 | 3.5 | 2.8 | 44.8 | 55.2 |
| CF5 | 5 | 8.4 | 8.2 | 8.1 | 46.3 | 53.7 |

*$N_p$ estimated from the MWs of each elution fraction in GPC curves and the arm precursor's using Eq. 2.
‡$N_g$ calculated from the contraction factors using Eq. 3.
†$N_{PF}$ estimated from the fractionation of GPC curves.
§$f_p$ and $f_c$ are the fractions of reacted BisAM with pendent double bonds and having both vinyl groups reacted in crosslinking for the core formation.

portions in the GPC traces. The peaks at the high MW portion were related to the s-PAMs, whereas the peak at the low MW end was attributed to residual (unreacted) linear PAM arm precursors produced in the first stage. The PAM precursors had MW about 62 kg/mol. As the incorporation of BisAM would not generate more precursor chains, the BisAM fraction was deducted from the MW of the s-PAM in estimating the number of arms from the total MW data. When the BisAM molar concentration was controlled at five times of the PAM precursors (AF5), a majority of the PAM precursors did not participate in the star formation. Only a small shoulder having a peak MW ~130 kg/mol appeared, attributing to two PAM precursors linked together, which were still linear in nature. Very small amount of s-PAMs was obtained in Run AF5. Increasing the BisAM content 20 times of PAM precursor (AF20) dramatically increased the intensity of the GPC peaks at the high MW portion, with reduction of the residual PAM precursor chains. The peak MW of the high MW portion in Run AF20 was ~250 kg/mol, suggesting the domination of 4-arm stars in the sample. Further increase in the BisAM/(PAM precursor) ratios to 30 (AF30) and 40 (AF40) favored the formation of stars having more arms. Runs AF30 and AF40 had the peak MWs at 390 and 960 kg/mol, respectively, equivalent to 6-arm and 14-arm stars. Using a deconvolution technique to subtract the PAM precursor portions (assuming a Gaussian distribution) from the total GPC traces, we found that the s-PAMs had respective $M_w$ and PDI as follows: 188 kg/mol and 1.0 for AF5, 268 kg/mol and 1.1 for AF20, 423 kg/mol and 1.3 for AF30, and 785 kg/mol and 1.7 for AF40.

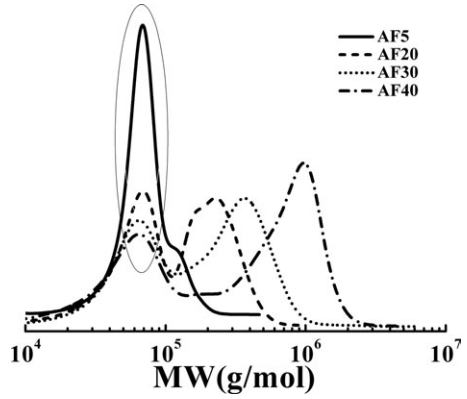


**Figure 1. GPC traces of s-PAM samples from Runs AF5–AF40 prepared by AF RAFT polymerization of AM with different BisAM contents at pH = 5, 60°C, $[AM]_0$ = 1 mol/L, and $[AM]_0/[CTA]_0/[I]_0$ = 600/1/0.5.**

**$[BisAM]_0/[CTA]_0$ = 5 (Run AF5), 20 (Run AF20), 30 (Run AF30), and 40 (Run AF40).**

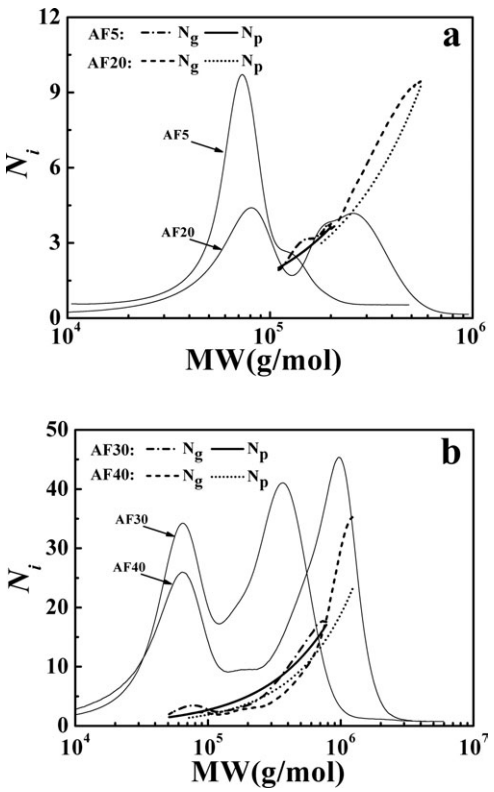


**Figure 2. The number of arms $N_i$ of the s-PAM samples from Runs AF5–AF40 prepared by AF RAFT polymerization as a function of MW of GPC elution fraction.**

**(a) $[BisAM]_0/[CTA]_0$ = 5 (Run AF5) and 20 (Run AF20); (b) $[BisAM]_0/[CTA]_0$ = 30 (Run AF30) and 40 (Run AF40). Solid lines are the $N_i$ estimated from the arm precursor, whereas dash lines refer to $N_i$ calculated from the contraction factor.**

The number of arms ($N$) of the star polymers can be estimated by comparison of their MWs with the arm precursor's. For a well-defined star polymer having narrow distribution, the actual $N$ can be calculated from its average MW.[21,77–79] When there existed a distribution in the number of arms, it would be more reliable to have the average $N$ estimated from the $N_i$ of each elution fraction in its GPC curve using the MW of each narrow slice ($M_{i,s}$) and the arm precursor's ($M_a$) with Eq. 2.

$$N_p = \sum_i N_i \cdot \omega(i) = \sum_i \frac{M_{i,s}}{M_a} \cdot \omega(i) \qquad (2)$$

where $\omega(i)$ is the weight fraction of each GPC slice with $MW_i$. The number of arms $N_i$ increased with MW as shown in Figure 2 for Runs AF5–AF40. The $N$ values calculated from Eq. 2 (denoted as $N_p$) for the AF s-PAMs are 1.4, 3.2, 5.3, and 12.1, respectively, tabulated in Table 3. Table 3 also gives the fractions of the incorporated BisAM monomers having both vinyl groups reacted during the core formation ($f_c$). About

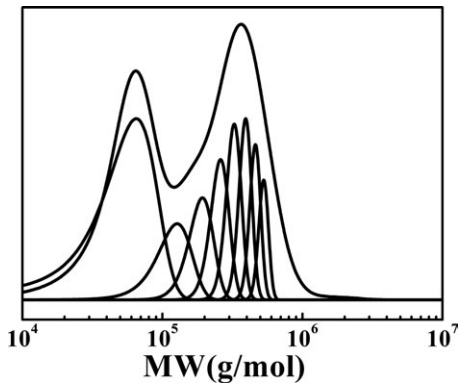


**Figure 3. Fractionation of GPC trace of the s-PAM sample from Run AF30 on the basis of stars having *i* number of arms *i* = 1,2,3,4, ...**

83.9–85.5% of the incorporated BisAM monomers in Runs AF20–AF40 had both vinyl groups crosslinked, while Run AF5 had only 57.2% incorporated BisAMs participated in the crosslinking reaction.

The intrinsic viscosities [$\eta$] for the AF s-PAMs were determined. The evolutions of intrinsic viscosity vs. MW for Runs AF5–AF40 are included in Appendix as Figure A1, with the linear PAM data as a reference. The contraction factor $g'$ was calculated and plotted against MW in Figure A2. As the current linear PAM arm precursors had low polydispersity indexes less than 1.1, the relationship between the contraction factor $g$ and the number of arms $N$ should obey Eq. 3 for regular stars with monodisperse arms of equal length joined together at one end such as the AF s-PAMs of this work.[76,80,81]

$$g_i = \frac{3N_i - 2}{N_i^2} \tag{3}$$

where $g$ was converted from $g'$ using Eq. 1. Figure 2 shows that the number of arms vs. MW data estimated from the MW ($N_i = M_{i,s}/M_a$) and the contraction factor (solved from $g_i$ in Eq. 3) agreed with each other very well. It can also be seen in Table 3 that the $N$ values estimated from the contraction factors (denoted as $N_g$) were in good agreement with the $N_p$ calculated from the MW data. The PAM samples produced from the AF approach were further proven to be star-shaped.

The s-PAM samples consisted of various star polymers and the linear arm precursors. The MW of the $i$-arm star polymers was $i$ times of the precursor's. The previous study showed that the precursor's MW followed a Gaussian distribution.[23] The s-PAM samples could, therefore, be fractionated into several subpopulations of the $i$-arm stars. Figure 3 shows an example of the fractionation of Run AF30 GPC trace. Figure 4 gives the weight fractions $\omega(i)$ of $i$-arms in the Runs AF5–AF40 samples, estimated by the fractionation of their GPC curves.

The characteristic feature of the $\omega(i)$ vs. $i$ curves followed the theoretical distribution for star polymers.[82] It can be seen that only 12.9 wt % of Run AF5 was 3- or 4-arm stars, while 87.1 wt % was unreacted precursor or two-arm coupling chains at BisAM/CTA = 5. With the increase of BisAM/CTA to 20, 30, and 40, the weight fractions of the stars having 3- and more arms reached 72.7, 84.0, and 94.9, respectively. The average arm numbers ($N_{PF}$) of the AF samples were also estimated from the peak fractionation and summarized in Table 2. A good agreement among the $N$ values estimated by the three different methods further supported the star structure of the PAMs synthesized by the AF approach.

### *Number of arms and distribution in the s-PAMs synthesized by CF approach*

The RAFT homopolymerization of BisAM could produce nanogels with crosslinked BisAM polymers. During the polymerization, the S=C(Z)S— groups were bound to the nanogels. The nanogels then functioned as a multifunctional CTA. The AM polymerization was mediated by these nanogel CTAs to prepare the star polymers (i.e., CF method).

Four different BisAM/CTA ratios of 1 (CF1), 3 (CF3), 5 (CF5), and 30 (CF30) (equivalent to BisAM/AM ratio 0.0017, 0.0050, 0.0083, and 0.050, respectively) were used to produce the s-PAM samples. When BisAM/CTA = 30, the gels formed by the crosslinked BisAM precipitated out in 40 min of the RAFT polymerization of BisAM, which could not be used for further AM polymerization. Nonprecipitated nanogels were produced with BisAM/CTA $\leq$ 5. 80.6% of BisAM reacted to form the nanogel after 3 h of polymerization in Run CF1, while the conversions were 65.7% in CF3 and 56.7% in CF5.

The CF1–CF5 nanogels were used as multifunctional RAFT agent in successive AM polymerization. All the runs reached overall conversions 96.4–97.6%. The CF1 s-PAM had $M_w$ of 108 kg/mol and PDI of 1.6, whereas the CF3 and CF5 samples had $M_w$ of 238 and 579 kg/mol and PDI of 1.7 and 2.4, respectively. The average number of RAFT units per nanogel for the CF s-PAMs could be estimated from the weight-average MW as 1.7 for CF1, 3.8 for CF3, and 9.2 for CF5.

Figure 5 shows the GPC traces of Runs CF1–CF5. In CF1 with BisAM/CTA = 1, the largest peak had MW about 65 kg/mol, which is linear single-armed PAM chains. All the s-PAM samples had a peak at 130 kg/mol, attributed to the coupling of 2 PAM arms. The peak at 65 kg/mol in CF3 and CF5 was minor. The formation of linear chains is due to the existence of the nanogels having 1 or 2 RAFT units, which cannot be avoided during the nanogel formation. The generation of linear chains was also found with —C(SR)=S functionalized nanogel RAFT CTA (in contrast to —SC(Z)=S of this work).[18,83] It is evident that s-PAMs having 3- or more arms were formed. The peak intensity at 190 kg/mol increased with the BisAM/CTA ratio. Small shoulders

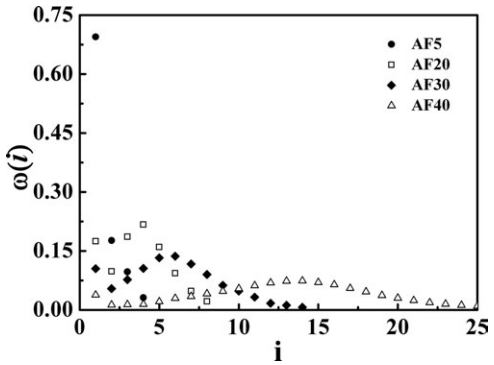


**Figure 4. Weight fraction distribution of *i*-arms, $\omega(i)$, in the s-PAM samples of AF5–AF40 synthesized with the AF approach using curve deconvolution of GPC trace as shown in Figure 3.**

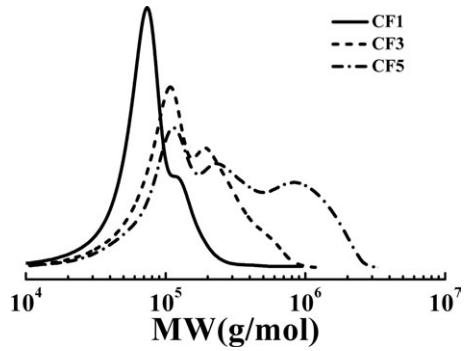


**Figure 5. GPC traces of s-PAM samples of Runs CF1–CF5 prepared by CF RAFT polymerization of AM with different ratios of BisAM at pH = 5, 60°C, $[AM]_0$ = 1 mol/L, and $[AM]_0/[CTA]_0/[I]_0$ = 600/1/0.5. $[BisAM]_0/[CTA]_0$ = 1 (Run CF1), 3 (Run CF3), and 5 (Run CF5).**

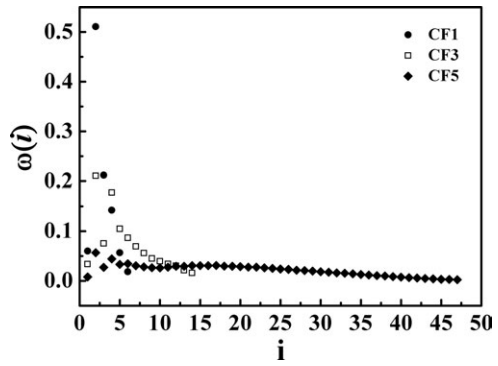


**Figure 7. Weight fraction distribution of *i*-arms $\omega(i)$ in the s-PAM samples of Run CF1-CF5 synthesized with the CF approach obtained from the curve deconvolution of GPC traces.**

appeared at the high MW end could also be resulted from star–star coupling reactions.[18,83] Further increase of BisAM/CTA favored the formation of s-PAMs having a higher number of arms. The GPC peak in Run CF5 had a high intensity at 250 kg/mol (4-arm). After removing the linear components at the peaks of 65 and 130 hg/mol from the GPC traces using the curve deconvolution technique, we found the weight-average MW and polydispersity index of the CF s-PAMs were 202 g/mol and 1.0 in Run CF1, 329 kg/mol and 1.2 in CF3 and 730 kg/mol and 1.9 in CF5, respectively.

The numbers of arms of the CF s-PAM samples were estimated from the comparison of their MWs and their linear PAM arm using Eq. 2. Figure 6 shows the evolution of $N_i$ with MW. The average numbers $N_p$ are presented in Table 3. The CF s-PAMs had the $N_p$ values 1.8, 3.3, and 8.4, respectively. The fractions of BisAM having both vinyl groups reacted ($f_c$) determined from NMR measurements were 53.7–59.4%, in the same range as of Run AF5.

From the intrinsic viscosities [$\eta$] and contraction factors for the CF s-PAMs (shown in Figures A3 and A4), the average numbers of arms $N_g$ were estimated using Eq. 3 and were also presented in Table 3. The $N_g$ values were 1.7 (CF1), 3.5 (CF3), and 8.2 (CF5), which were in good agreement with the $N_p$ of 1.8, 3.3, and 8.4 estimated from the MW data. Figure 6 also shows that the $N_i$ values estimated from the contraction factors at the high MW portion were lower than those from the MW data, indicating the presence of star–star coupling reactions.

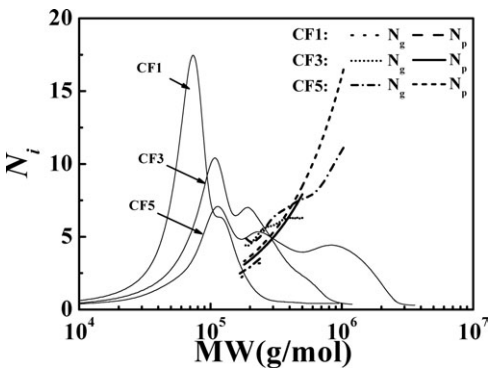


**Figure 6. Number of arms *N* of the s-PAM samples from Runs CF1-CF5 prepared by CF RAFT polymerization as a function of MW of GPC elution fraction.**

**$[BisAM]_0/[CTA]_0$ = 1 (Run CF1), 3 (Run CF3), and 5 (Run CF5). Solid lines are $N_i$ estimated from linear PAM arm, whereas dash lines refer to $N_i$ calculated from contraction factors.**

Figure 7 shows the weight fraction $\omega(i)$ of *i*-arms in Runs CF1–CF5 estimated by the curve deconvolution. It can be seen that Run CF1 contained 60.2% of single-arm linear chains, 28.5% of 2-arm linear chains, and 11.3% of 3- or 4-arm s-PAMs. An increase in BisAM/CTA to 3 (CF3) and 5 (CF5) promoted formation of the s-PAMs with more arms. Run CF3 possessed 45.3% of 3- and more arm stars with single-arm reduced to 23.6% and 2-arm slightly increased to 31.1%. Run CF5 had 83.6% of stars, 6.4% of single-arm, and 10.0% of 2-arm. The average numbers of arms $N_{PF}$ were estimated from the curve deconvolution and were included in Table 3. A good agreement between the *N* values from the curve deconvolution and the contraction factor was evident.

### *Branching density and distribution in the b-PAM's synthesized by BA and SB approaches*

Hyperbranched PAM samples (b-PAMs) were synthesized with batch (BA) and constant feeding (SB) approaches at three different BisAM/CTA ratios of 5 (SB5, BA5), 30 (SB30,[23] BA30[22]), and 40 (SB40) (equivalent to BisAM/AM = 0.0083, 0.050, and 0.067). Soluble PAM samples were obtained except for Run BA30. Run BA30 gelled in 65 min at an overall conversion 69%.[22] Runs SB5 to SB40 and BA5 had the overall conversion over 93.5% with almost all BisAM monomers incorporated. The b-PAM samples had weight-average MWs from 100 to 1290 kg/mol and PDI of 1.4–9.4. Both $M_w$ and PDI increased with the BisAM loading. The *g* and *g*′ data of the b-PAM samples are listed in Table 2, with *g*′ in the range of 0.283–0.915 and *g* in 0.194–0.889. The polymers having higher branching densities had lower *g*′ and *g* values at the same MW.

Figure 8 shows the GPC traces of the b-PAMs from Run SB5-40 and BA5. With BisAM/CTA = 5, the samples contained mainly either single primary chains (SB5, 62 kg/mol) or double primary chains (BA5, 130 kg/mol). Little branched PAMs were produced in Runs SB5 and BA5. With BisAM/CTA increased to 30 (SB30) and 40 (SB40), the GPC peaks at higher MW appeared, and more branched PAMs were

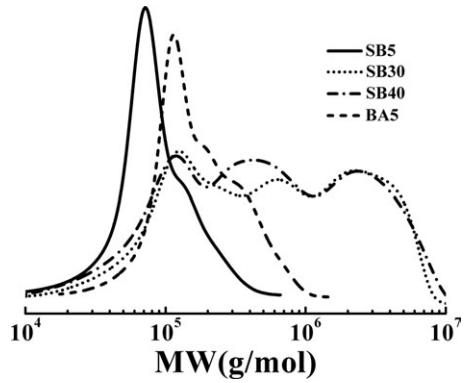


**Figure 8. GPC traces of b-PAM samples from Runs SB5–SB40 prepared by semibatch RAFT polymerization with BisAM constant feeding and Run BA5 by batch RAFT polymerization of AM with different BisAM/CTA ratios at pH = 5, 60°C, $[AM]_0$ = 1 mol/L, and $[AM]_0/[CTA]_0/[I]_0$ = 600/1/0.5. $[BisAM]_0/[CTA]_0$ = 5 (Runs SB5 and BA5), 30 (Run SB30),[23] and 40 (Run SB40).**

formed. The single primary chain peak diminished, although double primary chains were still significant.

The branching structures in the b-PAMs were found to be distributed randomly along primary chain backbones.[23] The

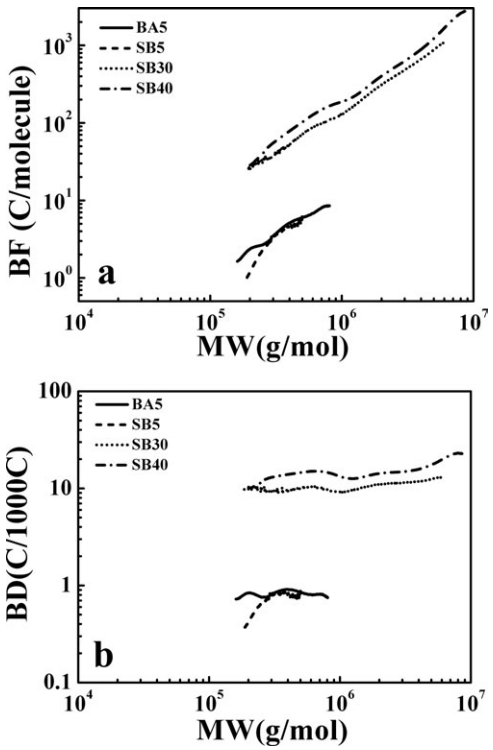


**Figure 9. BF (a) and BD (b) as a function of MW of GPC elution fraction in the b-PAM samples from Runs SB5–SB40 prepared by semibatch RAFT polymerization with BisAM constant feeding and Run BA5 by batch RAFT polymerization of AM with different BisAM/CTA ratios at pH = 5, 60°C, $[AM]_0$ = 1 mol/L, and $[AM]_0/[CTA]_0/[I]_0$ = 600/1/0.5.**

**$[BisAM]_0/[CTA]_0$ = 5 (Runs SB5 and BA5), 30 (Run SB30),[23] and 40 (Run SB40).**

**Table 4. BDs, CDs and Fractions of Polymerized BisAM Contributed to Their Formations Determined by $^1$H NMR, GPC with Triple-Detector and Fractionation of GPC Traces for b-PAMs**

| Run | $[BisAM]_0/[AM]_0$ | $BD_g$ (/1000C) | $BD_{PF}$* (/1000C) | $CD_{NMR}$† (/1000C) | $f_{pend}$‡ (%) | $f_{br}$‡ (%) | $f_{cyc}$‡ (%) |
|---|---|---|---|---|---|---|---|
| BA5 | 0.83 | 1.34 | 1.38 | 2.49 | 55.6 | 15.2 | 29.2 |
| SB5 | 0.83 | 0.39 | 0.42 | 3.24 | 57.6 | 6.0 | 36.4 |
| SB30[23] | 5.00 | 9.62 | 9.57 | 28.9 | 19.5 | 20.1 | 60.4 |
| SB40 | 6.67 | 13.1 | 13.5 | 35.2 | 17.1 | 22.2 | 60.7 |

*BD estimated from the fractionation of GPC curves.
†CD estimated from the amount of polymerized BisAM contributed to cyclization in b-PAMs.
‡$f_p$, $f_{br}$, and $f_{cyc}$ are the fractions of reacted BisAM contributed to pendent double bonds, branches, and cyclic structures, respectively.

branching frequency (BF, branching points per polymer molecule) and branching density (BD, per 1000 carbons) were estimated using Zimm–Stockmayer equation[76]

$$g = \left[\left(\sqrt{1+\left(\frac{\mathrm{BF}}{6}\right)}\right) + \frac{4\times \mathrm{BF}}{3\pi}\right]^{-1/2} \tag{4}$$

$$\mathrm{BD} = \frac{35,500\times \mathrm{BF}}{M}\times 2 \tag{5}$$

Figure 9 shows the BF and BD results of the s-PAMs. It can be seen that each MW elution in the b-PAM samples had a similar level of BDs, suggesting that the b-PAM samples had random branched distributions. Their average BDs estimated from $\sum_i \mathrm{BD}_i C_i / \sum_i C_i$ are presented in Table 4, where $C_i$ is the polymer concentration at each GPC elution fraction. The b-PAM samples had the average BDs from 0.39 to 13.1C/1000C. As the content of residual pendant double bonds ($c_p$) was about 0.49–1.02% of the total reacted vinyl groups, only 44–83% of the incorporated BisAM monomers contributed to either branching or cyclization. The cyclization densities (CDs, carbons per 1000 carbons) were estimated to be 2.49–35.2C/1000C. Among the reacted BisAM monomers, approximately 6.0–22.2% contributed to branching while 29.2–60.7% involved in cyclization.

A randomly branched polymer has a branch-on-branch structure and can be considered as an aggregation of $i$ primary linear chains.[23] Highly branched b-PAM samples

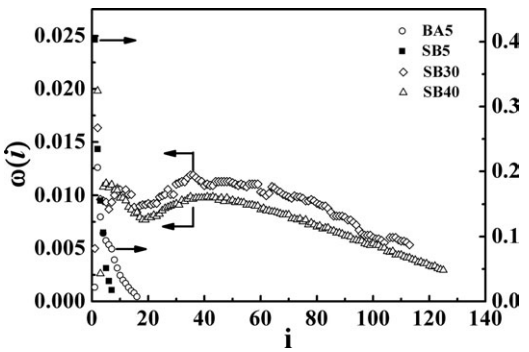


**Figure 10. Weight fraction distribution of $i$-arms $\omega(i)$ of the b-PAM samples from Runs SB5–SB40 synthesized by semibatch RAFT polymerization with BisAM constant feeding and Run BA5 by batch RAFT polymerization using the curve deconvolution of GPC traces.**

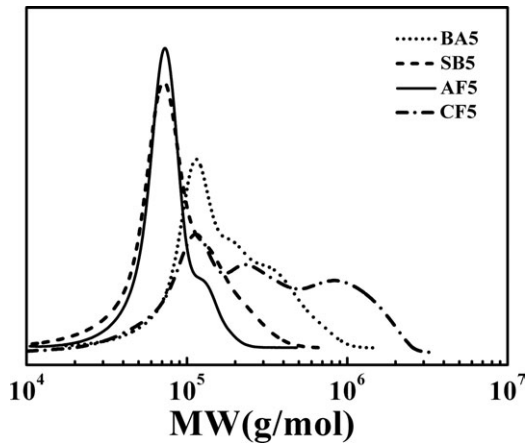


**Figure 11. GPC traces of the s-PAMs and b-PAMs synthesized by AF, CF, SB, and BA approaches at pH = 5, 60°C with the same recipe: $[AM]_0$ = 1 mol/L and $[AM]_0/[BisAM]_0/[CTA]_0/[I]_0$ = 600/5/1/0.5.**

contained a large number of primary chains. The MW of the primary chains used for the fractionation was 62 kg/mol. The multipeak MW distribution of the b-PAM samples could then be fractionated into several *i*-chain subpopulations through best fitting of GPC curves. Figure 10 shows the weight fractions $\omega(i)$ for SB5-40 and BA5 s-PAMs.

The characteristic feature of the $\omega(i)$ vs. $i$ curves matched the theoretical distribution for randomly branched polymers.[82] Using the BFs at various MWs in Figure 9a, the BF values for each *i*-chain subpopulation could be estimated. The average BDs estimated from $\sum_i \omega(\mathrm{i}) \cdot (35,500\mathrm{BF}_i/\mathrm{M}_i) \times 2$ are also presented in Table 4. A good agreement of the BD values from both GPC measurement and curve deconvolution further supported random branching distribution.

### *Effect of various feeding policies on PAM chain architectures*

Using the same recipe and temperature, we produced s- and b-PAMs via various monomer feeding policies. The number of arms or the BD was determined by the ratio of BisAM/CTA. Although high BisAM loading favored branching or arm formation, the success in the synthesis was mainly controlled by the BisAM feeding policy. When BisAM/CTA = 30 (equivalent to BisAM/AM = 0.05), only the AF and SB approaches produced soluble s-PAM (5.6 arms) and b-PAM samples (9.6 branches per 1000Cs) while the CF and BA systems gelled. The crosslinking reactions of BisAM in CF and BA could not be properly controlled. The AF and SB approaches appeared to be practical in producing the respective s-PAM and b-PAM at high $[BisAM]_0/[CTA]_0$ ratios or low CTA usages. Under the present experimental conditions, the critical gelation ratio of $[BisAM]_0/[CTA]_0$ was ~10 for the BA approach and 7 for the CF approach, respectively.

Lowering BisAM/CTA to 5 (or BisAM/AM to 0.0083) yielded soluble s- or b-PAMs in all the four approaches. Figure 11 shows the comparison of all the four feeding policies with BisAM/CTA = 5. For both AF and CF s-PAMs synthesized with BisAM/CTA = 5, the structures of the cross-linked cores were characterized by $^1$H NMR spectra. There were 42.8% double bonds pendant and 57.2% consumed for cross-linking in AF. In comparison, there were 46.3% pendant and 53.7% crosslinked in CF. Linear and star chains coexisted. However, the PAM precursor content dominated the linear chain population in Run AF5, although the majority of linear chains in Run CF5 were 2-arms. The MW of CF5 s-PAM (579 kg/mol) was much higher than AF5 (82 kg/mol). The number of arms in the CF5 s-PAM was about 8, whereas it was just about 1.5 in AF5. The b-PAMs were synthesized by the SB and BA approaches. The BD of SB5 b-PAM was 0.4C/1000Cs with MW about 100 kg/mol. In comparison, the BA5 b-PAM had the BD of 1.3C/1000Cs and MW about 204 kg/mol. Although the CF approach produced star polymers with more number of arms than the AF and the BA approach synthesized more branches than the SB at the same BisAM loading, the s-PAM and b-PAM products synthesized at high $[BisAM]_0/[CTA]_0$ ratios or low CTA usages appeared to be more feasible using the AF and SB approaches, respectively, as the CF and BA were prone to gel formation.

## Conclusion

s- and b-PAMs were synthesized by the RAFT copolymerization of AM and BisAM using different feeding policies of BisAM: AF, CF, constant feeding (SB), and batch (BA). The s-PAMs were prepared by sequentially polymerizing AM and BisAM in the AF or CF policies, whereas the b-PAMs were prepared by a constant feeding of BisAM into the AM polymerization system. The obtained samples were thoroughly characterized by various means. The numbers of arms of the s-PAMs were determined by triple-detector GPC measurements and a peak fractionation algorithm. The s-PAM samples prepared by the AF and CF policies had the *N* values in the range of 1.4–12.8 and 1.8–8.4, respectively. The BDs of the b-PAMs prepared by the SB and BA policies were in the range of 0.39–13.1C/1000Cs. With the high loading of BisAM (e.g., BisAM/CTA = 30) or low CTA usage, the CF and BA policies lead to gelation and were thus unable to produce soluble branched polymers, while the AF and SB policies yielded s-PAM having 5.6 arms and b-PAM 9.6C/1000Cs. With a lower BisAM loading (BisAM/CTA = 5), all the four policies became effective in preparation soluble branched PAM samples. The CF approach produced the s-PAMs with more number of arms than the AF, whereas the b-PAMs made by the BA approach had more branches compared to those with the SB. This work offered the first direct comparison among various monomer feeding policies in the preparation of branched PAMs via RAFT polymerization mechanism. It provided practical guidance to the selection of industrial processes in branched polymer production and fundamental insight to the molecular processes involved in RAFT polymerization with branching.

## Acknowledgments

This work is financially supported by National Natural Science Foundation of China (Grant 21074116 and Key Grant 20936006), Zhejiang Ministry of Science and Technology (Strategic Grant 2008C14087), Chinese State Key Laboratory of Chemical Engineering at Zhejiang University (Grant SKL-ChE-08D01), and the Program for Changjiang Scholars and Innovative Research Team in University in China (IRT0942).

## Literature Cited

1. Mortimer DA. Synthetic polyelectrolytes—A review. *Polym Int.* 1991;25:29–41.

2. Owen AT, Fawell PD, Swift JD, Farrow JB. The impact of polyacrylamide flocculant solution age on flocculation performance. *Int J Miner Process*. 2002;67:123–144.
3. Bolto B, Gregory J. Organic polyelectrolytes in water treatment. *Water Res*. 2007;41:2301–2324.
4. Hocking MB, Klimchuk KA, Lowen S. Polymeric flocculants and flocculation. *J Macromol Sci—Rev Macromol Chem Phys*. 1999; C39:177–203.
5. Wada T, Sekiya H, Machi S. Synthesis of high molecular-weight polyacrylamide flocculant by radiation polymerization. *J Appl Polym Sci*. 1976;20:3233–3240.
6. Brouillette F, Morneau D, Chabot B, Daneault C. Paper formation improvement through the use of new structured polymers and microparticle technology. *Pulp Paper Can*. 2004;105:31–35.
7. Brouillette F, Morneau D, Chabot B, Daneault C. A new microparticulate system to improve retention/drainage in fine paper manufacturing. *Appita J*. 2005;58:47–51.
8. Blanco A, Fuente E, Concepcion Monte M, Cortes N, Negro C. Polymeric branched flocculant effect on the flocculation process of pulp suspensions in the papermaking industry. *Ind Eng Chem Res*. 2009;48:4826–4836.
9. Gu L, Zhu S, Hrymak AN. Synthesis and flocculation performance of graft copolymer of *N*-vinylformamide and poly(dimethylaminoethyl methacrylate) methyl chloride macromonomer. *Colloid Polym Sci*. 2002;280:167–175.
10. Li D, Zhu S, Pelton RH, Spafford M. Flocculation of dilute titanium dioxide suspensions by graft cationic polyelectrolytes. *Colloid Polym Sci*. 1999;277:108–114.
11. Ma M, Zhu S. Grafting polyelectrolytes onto polyacrylamide for flocculation—1. Polymer synthesis and characterization. *Colloid Polym. Sci*. 1999;277:115–122.
12. Ma M, Zhu S. Grafting polyelectrolytes onto polyacrylamide for flocculation—2. Model suspension flocculation and sludge dewatering. *Colloid Polym Sci*. 1999;277:123–129.
13. Subramanian R, Zhu S, Pelton RH. Synthesis and flocculation performance of graft and random copolymer microgels of acrylamide and diallyldimethylammonium chloride. *Colloid Polym Sci*. 1999;277:939–946.
14. Mishra M, Kobayashi S.*Star and Hyperbranched Polymers*.New York:Marcel Dekker, Inc., 1999.
15. Voit BI, Lederer A. Hyperbranched and highly branched polymer architectures—synthetic strategies and major characterization aspects. *Chem Rev*. 2009;109:5924–5973.
16. Hadjichristidis N, Iatrou H, Pitsikalis M, Mays J. Macromolecular architectures by living and controlled/living polymerizations. *Prog Polym Sci*. 2006;31:1068–1132.
17. Blencowe A, Tan JF, Goh TK, Qiao GG. Core cross-linked star polymers via controlled radical polymerisation. *Polymer*. 2009; 50:5–32.
18. Barner-Kowollik C, Davis TP, Stenzel MH. Synthesis of star polymers using RAFT polymerization: what is possible? *Aust J Chem*. 2006;59:719–727.
19. Stenzel MH. Hairy core-shell nanoparticles via RAFT: where are the opportunities and where are the problems and challenges? *Macromol Rapid Commun*. 2009;30:1603–1624.
20. Gao H, Matyjaszewski K. Synthesis of functional polymers with controlled architecture by CRP of monomers in the presence of cross-linkers: from stars to gels. *Prog Polym Sci*. 2009;34:317–350.
21. Gao H, Matyjaszewski K. Synthesis of star polymers by a new "Core-First" method: sequential polymerization of cross-linker and monomer. *Macromolecules*. 2008;41:1118–1125.
22. Wang D, Li X, Wang W-J, Gong X, Li B-G, Zhu S. Kinetics and modeling of semi-batch RAFT copolymerization with hyperbranching. *Macromolecules*. 2012;45:28–38.
23. Wang W-J, Wang D, Li B-G, Zhu S. Synthesis and characterization of hyperbranched polyacrylamide using semibatch reversible addition-fragmentation chain transfer (RAFT) polymerization. *Macromolecules* 2010;43:4062–4069.
24. Bouhier MH, Cormack PAG, Graham S, Sherrington DC. Synthesis of densely branched poly(methyl methacrylate)s via ATR copolymerization of methyl methacrylate and ethylene glycol dimethacrylate. *J Polym Sci Part A: Polym Chem*. 2007;45:2375–2386.
25. Isaure F, Cormack PAG, Graham S, Sherrington DC, Armes SP, Butun V. Synthesis of branched poly(methyl methacrylate)s via controlled/living polymerisations exploiting ethylene glycol dimethacrylate as branching agent. *Chem Commun*. 2004;1138–1139.
26. Li W, Gao H, Matyjaszewski K. Influence of initiation efficiency and polydispersity of primary chains on gelation during atom transfer radical copolymerization of monomer and cross-linker. *Macromolecules*. 2009;42:927–932.
27. Li YT, Armes SP. Synthesis and chemical degradation of branched vinyl polymers prepared via ATRP: use of a cleavable disulfide-based branching agent. *Macromolecules*. 2005;38:8155–8162.
28. Li YT, Armes SP. Synthesis of model primary amine-based branched copolymers by pseudo-living radical copolymerization and post-polymerization coupling of homopolymers. *Macromolecules*. 2009;42:939–945.
29. Liu BL, Kazlauciunas A, Guthrie JT, Perrier S. One-pot hyperbranched polymer synthesis mediated by reversible addition fragmentation chain transfer (RAFT) polymerization. *Macromolecules*. 2005;38:2131–2136.
30. Poly J, Wilson DJ, Destarac M, Taton D. Synthesis of poly(vinyl acetate) nanogels by xanthate-mediated radical crosslinking copolymerization. *Macromol Rapid Commun*. 2008;29:1965–1972.
31. Rosselgong J, Armes SP, Barton W, Price D. Synthesis of highly branched methacrylic copolymers: Observation of near-ideal behavior using RAFT polymerization. *Macromolecules*. 2009;42:5919–5924.
32. Tao L, Liu JQ, Tan BH, Davis TP. RAFT synthesis and DNA binding of biodegradable, hyperbranched poly(2-(dimethylamino)ethyl methacrylate. *Macromolecules*. 2009;42:4960–4962.
33. Vo CD, Rosselgong J, Armes SP, Billingham NC. RAFT synthesis of branched acrylic copolymers. *Macromolecules*. 2007;40:7119–7125.
34. Wang AR, Zhu S. ESR study on diffusion-controlled atom transfer radical polymerization of methyl methacrylate and ethylene glycol dimethacrylate. *Macromolecules*. 2002;35:9926–9933.
35. Wang AR, Zhu S. Control of the polymer molecular weight in atom transfer radical polymerization with branching/crosslinking. *J Polym Sci Part A: Polym Chem*. 2005;43:5710–5714.
36. Yu Q, Gan Q, Zhang H, Zhu S.*Gelation kinetics of RAFT radical copolymerization of methacrylate and dimethacrylate*. In:Matyjaszewski K, editor.*Controlled/Living Radical Polymerization: Progress in RAFT*, DT, NMP & OMRP. Washington, DC: American Chemical Society. 2009; 1024:181–193.
37. Yu Q, Qin ZQ, Li JC, Zhu S. Diffusion-controlled atom transfer radical polymerization with crosslinking. *Polym Eng Sci*. 2008;48: 1254–1260.
38. Yu Q, Xu SH, Zhang HW, Ding YH, Zhu S. Comparison of reaction kinetics and gelation behaviors in atom transfer, reversible addition-fragmentation chain transfer and conventional free radical copolymerization of oligo(ethylene glycol) methyl ether methacrylate and oligo(ethylene glycol) dimethacrylate. *Polymer*. 2009;50:3488–3494.
39. Lord HT, Quinn JF, Angus SD, Whittaker MR, Stenzel MH, Davis TP. Microgel stars via reversible addition fragmentation chain transfer (RAFT) polymerisation—a facile route to macroporous membranes, honeycomb patterned thin films and inverse opal substrates. *J Mater Chem*. 2003;13:2819–2824.
40. Zheng GH, Pan CY. Preparation of star polymers based on polystyrene or polystyrene-b-*N*-isopropyl acrylamide) and divinylbenzene via reversible addition-fragmentation chain transfer polymerization. *Polymer*. 2005;46:2802–2810.
41. Adkins CT, Harth E. Synthesis of star polymer architectures with site-isolated chromophore cores. *Macromolecules*. 2008;41:3472–3480.
42. Licea-Claverie A, Alvarez-Sanchez J, Picos-Corrales LA, Obeso-Vera C, Flores MC, Munuel Cornejo-Bravo J, Hawker CJ.Frank CW. The use of the RAFT-technique for the preparation of temperature/pH sensitive polymers in different architectures. *Macromol Symp*. 2009;283–284:56–66.
43. Zheng Q, Zheng G, Pan CY. Preparation of nano-sized poly(ethylene oxide) star microgels via reversible addition-fragmentation transfer polymerization in selective solvents. *Polym Int*. 2006;55:1114–1123.
44. Angot S, Murthy KS, Taton D, Gnanou Y. Atom transfer radical polymerization of styrene using a novel octafunctional initiator: synthesis of well-defined polystyrene stars. *Macromolecules*. 1998;31:7218–7225.
45. Costa ROR, Vasconcelos WL, Tamaki R, Laine RM. Organic/inorganic nanocomposite star polymers via atom transfer radical polymerization of methyl methacrylate using octafunctional silsesquioxane cores. *Macromolecules*. 2001;34:5398–5407.
46. Heise A, Nguyen C, Malek R, Hedrick JL, Frank CW, Miller RD. Starlike polymeric architectures by atom transfer radical polymerization: templates for the production of low dielectric constant thin films. *Macromolecules*. 2000;33:2346–2354.

47. Matyjaszewski K. The synthesis of functional star copolymers as an illustration of the importance of controlling polymer structures in the design of new materials. *Polym Int*. 2003;52:1559–1565.
48. Matyjaszewski K, Miller PJ, Pyun J, Kickelbick G, Diamanti S. Synthesis and characterization of star polymers with varying arm number, length, and composition from organic and hybrid inorganic/organic multifunctional initiators. *Macromolecules*. 1999;32:6526–6535.
49. Wang JS, Greszta D, Matyjaszewski K. Atom transfer radical polymerization (ATRP): a new approach towards well-defined (co)polymers. *Polym Mater Sci Eng*. 1995;73:416–417.
50. Zhang W, Muller AHE. A "click chemistry" approach to linear and star-shaped telechelic POSS-containing hybrid polymers. *Macromolecules*. 2010;43:3148–3152.
51. Hussain H, Tan BH, Gudipati CS, Xaio Y, Liu Y, Davis TP, He CB. Synthesis and characterization of organic/inorganic hybrid star polymers of 2,2,3,4,4,4-hexafluorobutyl methacrylate and octa(aminophenyl)silsesquioxane nano-cage made via atom transfer radical polymerization. *J Polym Sci Part A: Polym Chem*. 2008;46:7287–7298.
52. Nese A, Mosnacek J, Juhari A, Yoon JA, Koynov K, Kowalewski T, Matyjaszewski K. Synthesis, characterization, and properties of starlike poly(*n*-butyl acrylate)-b-poly(methyl methacrylate) block copolymers. *Macromolecules*. 2010;43:1227–1235.
53. Boschmann D, Edam R, Schoenmakers PJ, Vana P. Characterization of Z-RAFT star polymerization of butyl acrylate by size-exclusion chromatography. *Macromol Symp*. 2008;275:184–196.
54. Boschmann D, Edam R, Schoenmakers PJ, Vana P. Z-RAFT star polymerization of styrene: comprehensive characterization using size-exclusion chromatography. *Polymer*. 2008;49:5199–5208.
55. Boschmann D, Maenz M, Poeppler A-C, Soerensen N, Vana P. Tracing arm-growth initiation in Z-RAFT star polymerization by NMR: the impact of the leaving R-group on star topology. *J Polym Sci Part A: Polym Chem*. 2008;46:7280–7286.
56. Chaffey-Millar H, Hart-Smith G, Barner-Kowollik C. Living star polymer formation (RAFT) studied via electrospray ionization mass spectrometry. *J Polym Sci Part A: Polym Chem*. 2008;46:1873–1892.
57. Chen W-X, Fan X-D, Huang Y, Liu Y-Y, Sun L. Synthesis and characterization of a pentaerythritol-based amphiphilic star block copolymer and its application in controlled drug release. *React Funct Polym*. 2009;69:97–104.
58. Hart-Smith G, Chaffey-Millar H, Barner-Kowollik C. Living star polymer formation: detailed assessment of poly(acrylate) radical reaction pathways via ESI-MS. *Macromolecules*. 2008;41:3023–3041.
59. Li Y, Zhang Y, Yang D, Hu J, Lu G, Huang X. Star-like PAA-g-PPO well-defined amphiphilic graft copolymer synthesized by ATNRC and SET-NRC reaction. *J Polym Sci Part A: Polym Chem*. 2010;48:2084–2097.
60. Liu J, Liu H, Jia Z, Bulmus V, Davis TP. An approach to biodegradable star polymeric architectures using disulfide coupling. *Chem Commun*. 2008;6582–6584.
61. Liu J, Tao L, Xu J, Jia Z, Boyer C, Davis TP. RAFT controlled synthesis of six-armed biodegradable star polymeric architectures via a 'core-first' methodology. *Polymer*. 2009;50:4455–4463.
62. Mori H, Ookuma H, Endo T. Poly(*N*-vinylcarbazole) star polymers and amphiphilic star block copolymers by xanthate-mediated controlled radical polymerization. *Macromolecules*. 2008;41:6925–6934.
63. Setijadi E, Tao L, Liu J, Jia Z, Boyer C, Davis TP. Biodegradable star polymers functionalized with beta-cyclodextrin inclusion complexes. *Biomacromolecules*. 2009;10:2699–2707.
64. Tao K, Lu D, Bai R, Li H, An L. A strategy for synthesis of ion-bonded supramolecular star polymers by reversible addition-fragmentation chain transfer (RAFT) polymerization. *Macromol Rapid Commun*. 2008;29:1477–1483.
65. Tao L, Kaddis CS, Loo RRO, Grover GN, Loo JA, Maynard HD. Synthesis of maleimide-end-functionalized star polymers and multimeric protein–polymer conjugates. *Macromolecules*. 2009;42:8028–8033.
66. Zhang W, Zhang W, Zhou N, Cheng Z, Zhu J, Zhu X. Synthesis and self-assembly behaviors of three-armed amphiphilic block copolymers via RAFT polymerization. *Polymer*. 2008;49:4569–4575.
67. Zhang W, Zhang W, Zhu J, Zhang Z, Zhu X. Controlled synthesis of pH-responsive amphiphilic A(2)B(2) miktoarm star block copolymer by combination of SET-LRP and RAFT polymerization. *J Polym Sci Part A: Polym Chem*. 2009;47:6908–6918.
68. Inglis AJ, Pierrat P, Muller T, Braese S, Barner-Kowollik C. Well-defined star shaped polymer-fullerene hybrids via click chemistry. *Soft Matter*. 2010;6:82–84.
69. McDowall L, Chen G, Stenzel MH. Synthesis of seven-arm poly(vinyl pyrrolidone) star polymers with lysozyme core prepared by MADIX/RAFT polymerization. *Macromol Rapid Commun*. 2008;29:1666–1671.
70. Chan JW, Yu B, Hoyle CE, Lowe AB. Convergent synthesis of 3-arm star polymers from RAFT-prepared poly(*N*,*N*-diethylacrylamide) via a thiol-ene click reaction. *Chem Commun*. 2008;4959–4961.
71. Inglis AJ, Sinnwell S, Davis TP, Barner-Kowollik C, Stenzel MH. Reversible addition fragmentation chain transfer (RAFT) and hetero-Diels–Alder chemistry as a convenient conjugation tool for access to complex macromolecular designs. *Macromolecules*. 2008;41:4120–4126.
72. Jesberger M, Barner L, Stenzel MH, Malmstrom E, Davis TP, Barner-Kowollik C. Hyperbranched polymers as scaffolds for multifunctional reversible addition-fragmentation chain-transfer agents: a route to polystyrene-core-polyesters and polystyrene-block-poly(butyl acrylate)-core-polyesters. *J Polym Sci Part A: Polym Chem*. 2003;41:3847–3861.
73. Brandrup J, Immergut EH, Grulke EA.*Polymer Handbook*, 4th ed.New York:Wiley, 1999.
74. Kong L-Z, Sun M, Qiao H-M, Pan CY. Synthesis and characterization of hyperbranched polystyrene via click reaction of AB(2) macromonomer. *J Polym Sci Part A: Polym Chem*. 2010;48:454–462.
75. Wang W-J, Kharchenko S, Migler K, Zhu S. Triple-detector GPC characterization and processing behavior of long-chain-branched polyethylene prepared by solution polymerization with constrained geometry catalyst. *Polymer*. 2004;45:6495–6505.
76. Zimm BH, Stockmayer WH. The dimensions of chain molecules containing branches and rings. *J Chem Phys*. 1949;17:1301–1314.
77. Gao H, Matyjaszewski K. Arm-first method as a simple and general method for synthesis of miktoarm star copolymers. *J Am Chem Soc*. 2007;129:11828–11834.
78. Gao H, Matyjaszewski K. Synthesis of low-polydispersity miktoarm star copolymers via a simple "Arm-First" method: macromonomers as arm precursors. *Macromolecules*. 2008;41:4250—4257.
79. Lapienis G. Star-shaped polymers having PEO arms. *Prog Polym Sci*. 2009;34:852–892.
80. Berry GC, Orofino TA. Branched polymers. 3. Dimensions of chains with small excluded volume. *J Chem Phys*. 1964;40:1614–1621.
81. Burchard W. *Advances in Polymer Science*. Heidelberg: Springer, 1999.
82. Zhu S. Analytical functions for molecular weight and branching distributions in star-, comb-, and random-branched polymers. *Macromolecules*. 1998;31:7519–7527.
83. Stenzel-Rosenbaum M, Davis TP, Chen V, Fane AG. Star-polymer synthesis via radical reversible addition-fragmentation chain-transfer polymerization. *J Polym Sci Part A: Polym Chem*. 2001;39:2777–2783.

## Appendix

See Figures A1–A4.

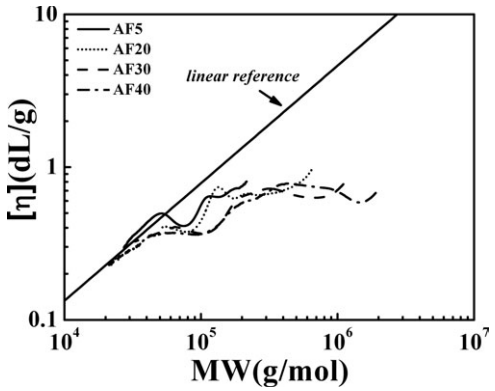


**Figure A1. Intrinsic viscosity ([$\eta$]) of Runs AF5–AF40 b-PAM samples prepared by AF RAFT polymerization of AM with different ratios of BisAM at pH = 5, 60°C, $[AM]_0$ = 1 mol/L, and $[AM]_0/[CTA]_0/[I]_0$ = 600/1/0.5.**

**$[BisAM]_0/[CTA]_0$ = 5 (Run AF5), 20 (Run AF20), 30 (Run AF30), and 40 (Run AF40).**

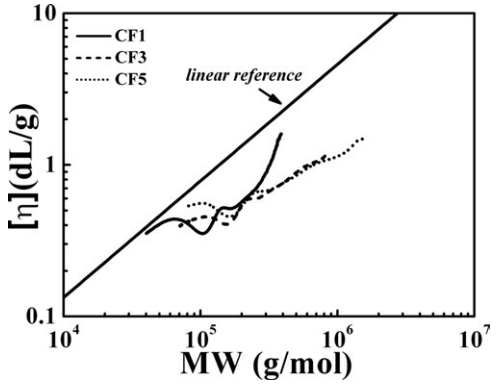


**Figure A3. Intrinsic viscosity ([$\eta$]) of Runs CF1–CF5 b-PAM samples prepared by CF RAFT polymerization of AM with different ratios of BisAM at pH = 5, 60°C, $[AM]_0$ = 1 mol/L, and $[AM]_0/[CTA]_0/[I]_0$ = 600/1/0.5.**

**$[BisAM]_0/[CTA]_0$ = 1 (Run CF1), 3 (Run CF3), and 5 (Run CF5).**

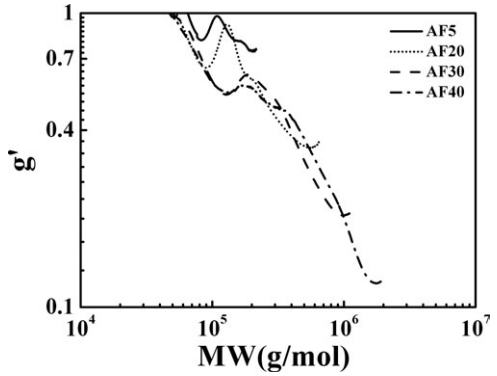


**Figure A2. Contraction factor $g'$ of Runs AF5–AF40 b-PAM samples prepared by AF RAFT polymerization of AM with different ratios of BisAM at pH = 5, 60°C, $[AM]_0$ = 1 mol/L, and $[AM]_0/[CTA]_0/[I]_0$ = 600/1/0.5.**

**$[BisAM]_0/[CTA]_0$ = 5 (Run AF5), 20 (Run AF20), 30 (Run AF30), and 40 (Run AF40).**

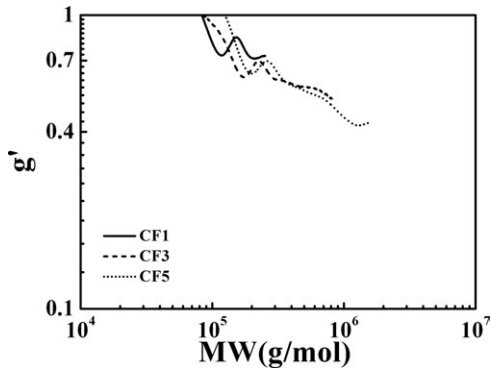


**Figure A4. Contraction factor $g'$ of Runs CF1–CF5 b-PAM samples prepared by CF RAFT polymerization of AM with different ratios of BisAM at pH = 5, 60°C, $[AM]_0$ = 1 mol/L, and $[AM]_0/[CTA]_0/[I]_0$ = 600/1/0.5.**

**$[BisAM]_0/[CTA]_0$ = 1 (Run CF1), 3 (Run CF3), and 5 (Run CF5).**

*Manuscript received Feb. 27, 2012, and revision received Jun. 5, 2012.*